J Mater Sci (2010) 45:5482–5489
DOI 10.1007/s10853-010-4605-2

Effect of strain rate on quasistatic tensile flow behaviour of solution annealed 304 austenitic stainless steel at room temperature

Amrita Kundu · Pravash Chandra Chakraborti

Received: 8 September 2009 / Accepted: 6 May 2010 / Published online: 21 May 2010

Abstract Room temperature tensile test results of solution annealed 304 stainless steel at strain rates ranging between 5×10^{-4} and 1×10^{-1} s^{-1} reveal that with increase in strain rate yield strength increases and tensile strength decreases, both maintaining power–law relationships with strain rate. The decrease in tensile strength with increasing strain rate is attributed to the lesser amount of deformation-induced martensite formation and greater role of thermal softening over work hardening at higher strain rates. Tensile deformation of the steel is found to occur in three stages. The deformation transition strains are found to depend on strain rate in such a manner that Stage-I deformation (planar slip) is favoured at lower strain rate. A continuously decreasing linear function of strain rate sensitivity with true strain has been observed. Reasonably good estimation for the stress exponent relating dislocation velocity and stress has been made. The linear plot of reciprocal of strain rate sensitivity with true strain suggests that after some critical amount of deformation the increased dislocation density in austenite due to the formation of some critical amount of deformation-induced martensite plays important role in carrying out the imposed strain rate.

A. Kundu · P. C. Chakraborti (✉)
Metallurgical and Material Engineering Department, Jadavpur University, Kolkata 700 032, India
e-mail: p_chakraborti@hotmail.com

Present Address:
A. Kundu
School of Metallurgy and Materials, University of Birmingham, Birmingham B152TT, UK

Introduction

Different grades of austenitic stainless steels (ASS) find extensive applications for their very good combination of corrosion resistance, high- and low-temperature strength and ductility and excellent weldability. The high work hardening rate and ductility in the annealed state allow the application of ASS for severe forming operations. However, some austenitic stainless steel grades are metastable and prone to deformation-induced phase change from the initial face-centred cubic austenite (γ) to body-centred cubic martensite (α) upon plastic deformation. The extent of such transformation primarily depends upon composition and temperature [1, 2]. Other factors that can affect the extent of transformation are plastic strain, strain rate, stress state, strain path and also grain size [1, 3, 4]. Martensite being stronger than austenite, it is expected that the formation of deformation-induced martensite (DIM) in austentic stainless steel would result higher strength along with higher ductility if martensite formation occurs prior to severe strain localisation [5, 6].

Many investigators studied the effect of deformation mode on martensitic transformation in austenitic stainless steel at room temperature and concluded differing results. Powell et al. [7] investigated the effect of temperature (10–293 K), strain rate and deformation modes such as tension, torsion and compression on the strain-hardening characteristics of type 301 and 304 austenitic stainless steel and correlated them with of volume fraction of martensite. Their observation suggests that the deformation mode substantially affects the transformation of martensite in the plastic range, and uniaxial tension enhances martensite formation in comparison to either compression or torsion. On the other hand, Okutani et al. [8] reported that in 304 austenitic stainless steel volume fraction of martensite at

room temperature is higher under uniaxial compression than that under tension and it increases with imposition of hydrostatic stress. Hecker et al. [9] found that more martensite formed in 304 steel during balanced biaxial tension than during uniaxial tension. Finally, Iwamoto et al. [10] showed that the magnitude of the average volume fraction of martensite for compression is higher than for tension in the initial stage of the deformation, and then the relation is reversed in the high strain region.

Considering the mechanical properties of austenitic stainless steels, the main effect of strain rate has been shown to be the adiabatic heating that reduces DIM formation at high strain rates [7, 11]. Bressanelli and Moskowitz [11] clearly demonstrated this effect in alloys 301 and 304 by applying various strain rates during tensile testing. These investigators showed that the best elongation was associated with the formation of about 50 vol.% martensite.

Although quasi-static tensile tests of different materials usually done at strain rates ranging between 1×10^{-5} and 1×10^{-2} s^{-1} are generally regarded as isothermal process, there may also be the retention of deformation heat in austenitic stainless steel specimens because of very low thermal conductivity of ASS. The rise in specimen temperature due to retention of deformation heat and the formation of DIM alter the tensile flow behaviour of metastable austenitic stainless steels [3, 6, 9, 12–14]. Such alteration may also take place in the quasi-static tensile flow behaviour of austentic stainless steels.

The effect of strain rate on tensile flow behaviour of any material at constant strain and temperature is characterised by its strain rate sensitivity (m). It is reported that with increase in strain rate flow stress increases resulting in an increase of yield strength and tensile strength with simultaneous lowering in ductility [3]. In fact, m reflects the plastic flow behaviour of different metals taking account of dislocation density, dislocation velocity and the barriers against dislocation movement. Hence, it is natural to expect that there must be some relationship of m with true strain. However, till date very few reports are available that describe the variation of m with the amount of strain. Existing reports [13, 15–17], however, reveal different nature of variation of m with true strain depending upon the material system. For example, Picu et al. [15] observed a negative strain rate sensitivity (SRS) at room temperature for all strains in case of commercial variety AA5182-O grade aluminium alloy, but without any specific trend. The negative SRS of the material is caused by smaller scale phenomena associated with interactions between solute and dislocations, referred to as dynamic strain ageing (DSA). Stewe and Les [16] reported an increasing trend in the variation of m with resolved shear strain for high purity aluminium, Lee and Lin [13] observed m to decrease with true strain for 304L stainless steel and Chiou et al. [17] observed minor increase of m in Fe–Mn–Al system. It is important to note here that the results [13, 17] are for experiments carried out at strain rates much higher than that prescribed for quasi-static deformation studies. Hence, a direct extrapolation of the dynamic test results to much lower strain rate situation might lead to wrong interpretation about the tensile flow behaviour of a material undergoing quasi-static deformation.

The objective of the present study is to investigate the effect of strain rate on quasi-static tensile flow behaviour of a commercial variety solution annealed austenitic stainless steel and to see how SRS of the investigated steel varies with the amount of deformation.

Experimental

The present study was done on a commercial variety 304 austenitic stainless steel. Chemical composition (wt%) of the investigated steel was: Fe–0.06 C–1.31 Mn–8.70 Ni–18.20 Cr–0.57 Si–0.005 S–0.025 P. Cylindrical specimen blanks of 110.0 mm in length were solution annealed at 1050 ± 2 °C for 45 min and then quenched in water.

Specimen for developing microstructure was obtained by transverse sectioning of a solution annealed specimen blank. After usual metallographic polishing, the specimen was etched with glyceregia and observed under an inverted optical microscope (Leica DMILM). Digital image of the microstructure was captured with the help of a digital camera (Leica DC300) interfaced with a personal computer.

Specimens used for tensile testing were uniform in diameter ($\Phi = 6.00$) and of very good surface finish with two gauge markings at 30 mm apart. Displacement controlled tensile tests at six different initial engineering strain rates ranging between 5×10^{-4} and 1×10^{-1} s^{-1} were done at room temperature (~25 °C) until fracture in a servohydraulic universal testing machine, Instron 8501 of ±100 kN load capacity. Tensile fracture surfaces of some specimens tested at different strain rates were observed in a scanning electron microscope (Make; Jeol, Model: JSM 6360) under secondary electron imaging mode.

As it is well known that this actuator displacement does not truly reflect the specimen deformation, the load-elongation data obtained from experiments under displacement control mode were analysed for knowing the actual specimen strain at different strain rates. Elastic deformation of the machine constitutes some fraction of the total actuator displacement. The amount of this elastic deformation of the machine depends upon load and machine stiffness, which is constant. Hence to find the actual specimen deformation, it is required to make necessary stiffness correction.

A separate test with the same material has been done to know the machine stiffness. This was done by attaching an extensometer of 25.00 mm gauge length to the specimen surface while testing at a strain rate of 5×10^{-4} s^{-1}. During this test, both actuator displacement and extensometer strain (specimen strain) was monitored. The difference between the actuator displacement and the specimen elongation obtained by multiplying extensometer strain with extensometer gauge length was plotted against every load point. In doing so, a linear curve was obtained which passed through the origin of the plot. The slope of this curve (=80 kN/mm) was the machine stiffness. Once the machine stiffness was obtained, the specimen strain was obtained using the following relationship:

$$\text{Specimen strain} = \left[\left\{\text{Actuator displacement} - \text{load } (P)/\text{Machine stiffness } (K)\right\}/30.00\right].$$

Results and discussion

Microstructure of solution annealed steel

Microstructure of the steel (Fig. 1) consists of polygonal grains of austenite with annealing twins characteristic of austenitic stainless steel interspersed in some grains. The two-dimensional nominal grain diameter was determined by various methods (linear intercept, planimetric and three circle). The approximate ASTM grain size is found as 4.5. The average Vickers hardness of the steel taken under 1 kg load is 161 kg/mm^2.

Tensile properties

Engineering stress–strain curves of the steel drawn after necessary stiffness ($K = 80$ kN/mm) correction of load-elongation data at different initial engineering strain rates are shown in Fig. 2. The stiffness corrected tensile test

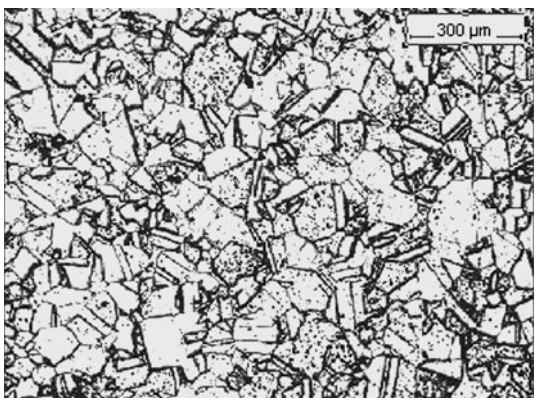

Fig. 1 Optical microstructure of solution annealed 304 steel

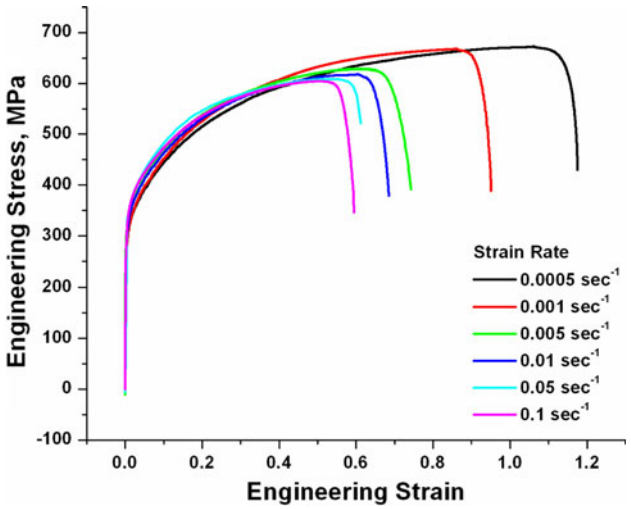

Fig. 2 Stress–strain curves at different initial engineering strain rates

results shown in Table 1 reveal that while yield strength (0.2% strain offset) increases with increase in strain rate, tensile strength is gradually decreased contrary to the common knowledge, both following power relationships with strain rate as: YS (MPa) $= 311.67\ \dot{e}^{-0.018}$ ($R^2 = 0.97$) and TS (MPa) $= 578.38\ \dot{e}^{-0.018}$ ($R^2 = 0.96$). Table 1 further reveals that all the ductility parameters, total and uniform elongations (e_t, e_u, ε_u) and reduction of area (RA) are continuously decreased with increase in strain rate.

The simultaneous lowering of tensile strength and ductility with increase in strain rate is rationalised by considering two opposite phenomena involved during plastic deformation [13, 17–19]: work hardening and thermal softening. Although work hardening is related to the difficulties associated with dislocation movement by different types of barriers, thermal softening occurs because of the difficulty for dissipation of heat to the surrounding material and environment during adiabatic deformation with consequent rise in specimen temperature, especially for materials with low thermal conductivity, e.g. austenitic stainless steels [13, 17]. In general, tensile flow behaviour during the course of adiabatic deformation is the effect of thermal–mechanical coupling and the final flow curve is the result of the competition between the rate of work hardening and the rate of thermal softening.

Figure 3 shows the estimated rate of change (rise) in specimen temperature with strain rate at maximum load point. The estimation for change in temperature has been done according to the equation [13]: $\Delta T = (1/\rho C_p) \int \sigma d\varepsilon$, where, ΔT is the temperature rise, ρ the density, C_p the heat capacity, σ the true stress and ε the true strain. Here, it has been assumed that complete adiabatic condition prevails for all strain rates, which, however, is most unlikely for all applied stain rates. In evaluating the above integral tensile flow curves ($\sigma - \varepsilon$) up to the maximum load point has

Table 1 Tensile properties of solution annealed 304 steel at different strain rates

Initial engineering strain rate (s^{-1})	0.2% Offset yield strength (MPa)	Tensile strength (MPa)	% Strain			% RA	True fracture ductility (%)
			e_t	e_u	ε_u		
5×10^{-4}	268.0	672.10	108.30	99.60	74.00	85.43	192.62
1×10^{-3}	277.0	649.50	95.70	87.76	63.00	80.75	164.76
5×10^{-3}	283.0	628.46	75.00	66.52	51.00	78.70	154.46
1×10^{-2}	287.0	618.00	68.50	61.60	48.00	75.32	139.92
5×10^{-2}	291.4	611.20	61.30	56.83	45.00	75.00	138.63
1×10^{-1}	298.3	608.40	59.40	52.20	42.70	67.30	111.78

been described by a polynomial with correlation coefficient 0.98 and above. It is observed from Fig. 3 that specimen temperature increases very rapidly for strain rates of 5×10^{-2} and above, and reaches to ~72 °C. Although no attempt has been made to measure the actual rise in specimen temperature, the estimated rise in temperature in the present case is found very much similar to that reported by Talolen et al. [3].

In case of austenitic stainless steel formation of Lomer–Cottrell barriers during plastic deformation is most prevalent because of its FCC crystal structure. The effectiveness of Lomer–Cottrell barrier in retarding dislocation movement is one of the most deciding factors for work hardening behaviour of FCC metals. Besides Lomer–Cottrell barriers, formation of DIM in metastable austenitic stainless steels is another source for hardening [5, 13, 20]. In addition to behaving as a strengthening phase, the formation of DIM also enhances ductility by raising the work hardening capacity of the steel [5, 20]. It is, therefore, logical to assume that any phenomenon that reduces work hardening either by lowering the effectiveness of Lomer–Cottrell barriers or by lowering the amount of DIM would lower tensile strength and ductility both.

Although in the present study, the formation of DIM as a function of strain rate and amount of deformation has not been studied in detail, except metallographic verification about the formation of DIM in some tensile deformed specimens one of the present authors (PCC) and others [21]

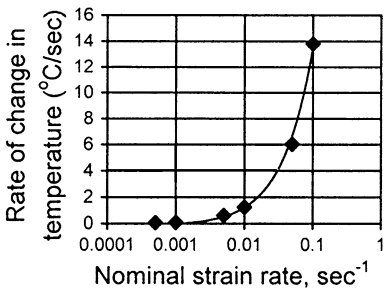

Fig. 3 Estimated rate of change in specimen temperature with strain rate

have recently shown that with increase in strain rate within quasi-static domain the formation of DIM in 304LN steel is commenced at an early stage of deformation and the extent of martensite is lowered with increasing strain rate. Investigations on 304L and 301LN steels carried out by other investigators [3, 6] also showed that at any fixed strain level martensite formation is lowered on increasing the strain rate within quasi-static domain. Optical microstructures of 20% tensile deformed specimens shown in Fig. 4a, b reveal the effect of increasimg strain rate by an order of two on DIM formation within quasistatic domain. On comparing these two micrographs, it is qualitatively revealed that lesser amount of martensite forms when deformation is done at higher strain rate. Thus, lesser amount of martensite formation and likelihood breaking down of the Lomer–Cottrell barriers, both expectedly due to increase in specimen temperature arising out of retention of deformation heat, seem to lower the work hardening of the present steel with gradual increase in strain rate. However, it cannot be confirmed at this stage whether a *sudden* temperature rise of ~72 °C even for assumed complete adiabatic heating even straining at 5×10^{-2} and 10^{-1} s^{-1} has any influence in overcoming Lomer–Cottrell barriers by gliding dislocations. Nevertheless, it is expected that increasing the strain rate would enhance dislocation mobility because of increased temperature and thereby reduce the work hardeanability of the steel [6, 17].

Besides enhanced dislocation mobility, the rise in specimen temperature is likely to give way for thermal softening with direct bearing on localised deformation [13, 19]. In the present study, thermal softening effect is revealed on the tensile fracture morphology. Representative tensile fracture surfaces shown in Fig. 5a–c reveals gradual enlargement of voids with increasing strain rate. This observation is very much in conformity to that reported by Das et al. [22]. Das et al. conducted a detail study on void morphology and distribution of voids formed in 304LN steel as a function of strain rate, while deformation is mostly carried out within quasi-static domain. In that study, it has been shown that the average circular diameter of voids increases and void number density is

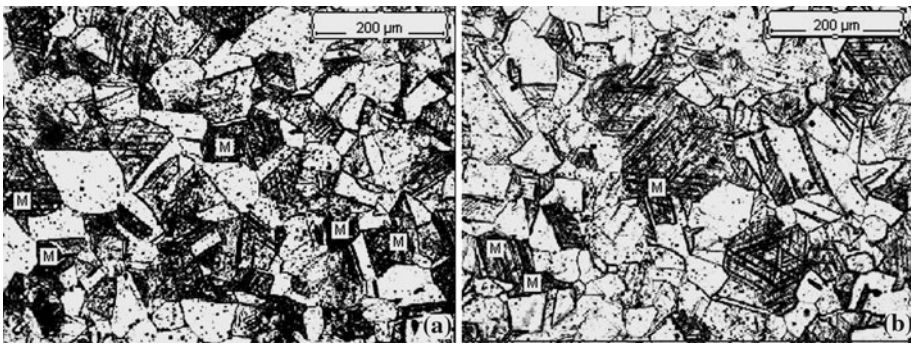

Fig. 4 Optical microstructure of after 20% tensile deformed specimens at two different strain rates: **a** 10^{-4} s^{-1} and **b** 10^{-2} s^{-1}

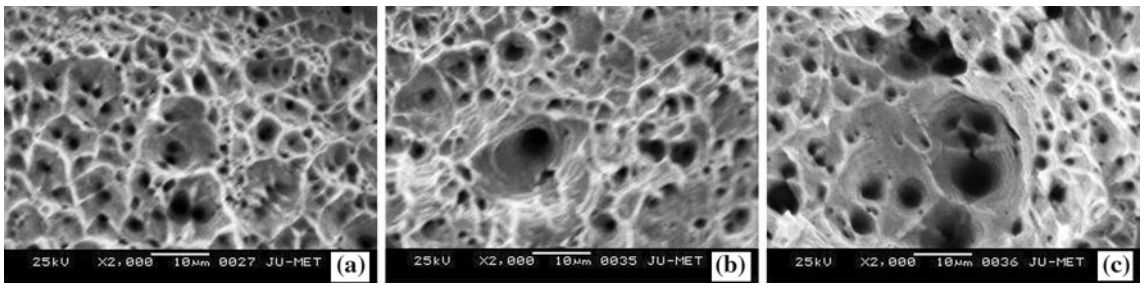

Fig. 5 Scanning electron fractographs of tensile fractured specimens: **a** 5×10^{-4} s^{-1}, **b** 5×10^{-3} s^{-1}, and **c** 5×10^{-2} s^{-1}

decreased with increasing strain rate. It is, therefore, concluded that with increasing strain rate even within quasi-static domain thermal softening effects predominate over work hardening and thereby lower both tensile strength and ductility of solution annealed 304 steel. Lichtenfeld et al. [6] also observed that with increase in strain rate within quasi-static domain yield strength increased with simultaneous lowering of tensile strength and ductility in case of 304L steel. These investigators explained their findings in terms of reduced formation of DIM with increasing strain rate. Talonen et al. [3] also made similar observation in their study with 304 steel.

Work hardening

To get the true picture about strain rate dependent work hardening response of the steel, tensile flow curves up to the point of peak load have been analysed by semilogarithmic plotting of true stress (σ) and true plastic strain (ε_p). In each of these plots, three different segments have been identified through power–law curve fitting (Hollomon relationship): $\sigma = k\varepsilon_p^n$, where k is the strength coefficient and n is the work hardening parameter. In fitting the power–law curves, the range of plastic strain has been increased in steps of 0.1% as long as the regression coefficient (R^2) value is greater than 0.98.

These three segments dividing the complete flow curve up to the point of maximum load correspond to three different deformation stages of the investigated steel. Work hardening parameters (n_1, n_2, n_3) associated with these deformation stages are shown in Table 2. The strength coefficient and work hardening parameter (k, n) of the steel for different strain rates obtained after fitting the complete flow curves with a single power–law curve are also included in Table 2.

Many investigators [3, 6, 14, 23, 24] have earlier reported that tensile deformation of different austenitic stainless steels occur in a number of stages. Similar multistage deformation has also been observed for copper and nickel, both belonging to fcc system [25, 26]. However, it is important to note here that Stage-I deformation that has been identified in these studies including the present one is different from the Stage-I deformation behaviour of fcc single crystal where work hardening rate is extremely low and the term "easy glide" or "laminar flow" is referred to characterise Stage-I deformation of single crystal. It is worthwhile to mention here the observation of Feaugas [23] on polycrystalline 316L stainless steel. Feaugas showed that during Stage-I deformation of polycrystalline 316L stainless steel more than 50% grains were activated for single slip system and consequently the grains behaved more as a single crystal oriented for single slip than for multiple slip. Further the extent of Stage-I deformation is reported to be much lower compared to the present finding (Table 2) and depends upon grain size and stacking fault energy [23, 24]. However, the effect of strain rate over the extent of Stage-I deformation has not been reported elsewhere. In the present study, the strain regime corresponding to Stage-I deformation with minimum work hardening parameter (n_1) is found to decrease with increasing strain

Table 2 Work hardening parameters of solution annealed 304 steel at different strain rates

Initial engineering strain rate (s^{-1})	Work hardening parameter (n)			$(n_1 + n_2 + n_3)/3$	n	Transition strain (%) (Stage I to II)	Transition strain (%) (Stage II to III)	Strength coefficient (MPa)
	n_1	n_2	n_3					
5×10^{-4}	0.142	0.342	0.620	0.368	0.395	5.40	23.50	1365
1×10^{-3}	0.149	0.349	0.588	0.362	0.387	5.04	22.78	1356
5×10^{-3}	0.139	0.307	0.492	0.313	0.316	4.45	20.50	1181
1×10^{-2}	0.140	0.309	0.470	0.306	0.313	4.40	18.04	1163
5×10^{-2}	0.135	0.304	0.435	0.291	0.261	3.90	16.45	1073
1×10^{-1}	0.123	0.248	0.418	0.263	0.283	3.80	15.00	1101

rate meaning that multiple slip/cross slip activation quickly sets in so to accommodate higher strain rate.

In the present study, Stage-II hardening exponent (n_2) is found to vary in the range of 0.30 to 0.35 except for testing at 10^{-1} s^{-1} ($n_2 = 0.248$). It is believed that rapid rise in specimen temperature for testing at 10^{-1} s^{-1} facilitates cross slipping of dislocations easily and thereby lowers work hardening. Very high Stage-III hardening exponent (n_3) is attributed to the formation of martensite [20]. An increase in work hardening rate due to formation of DIM is also reported in literature [3, 27–30]. Here, it is interestingly observed that higher is the strain rate lower is the n_3 value. This is attributed to the reduced amount of martensite formation with increasing strain rate; a direct consequence of increased specimen temperature with increasing strain rate. On plotting the transition strains as a function of strain rate, it is found that the transition strains gradually decrease with increase in strain rate following power relationships ($R^2 > 0.97$). The data for transition strains indicate that while planer slip activity (Stage-I) in solution annealed 304 steel is favoured at low strain rate; formation of DIM initiates early with increasing strain rate in conformity to that reported by Das et al. [22].

Strain rate sensitivity

Figure 6 shows that over the strain (ε) interval of 5 to 40% flow stress (σ) increases with increase in instantaneous true strain rate ($\dot{\varepsilon}$) following power relationships ($R^2 = 0.96$ to

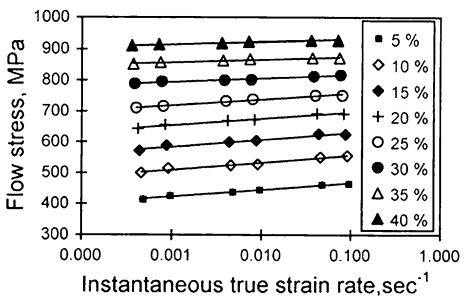

Fig. 6 Effect of strain rate on flow stress

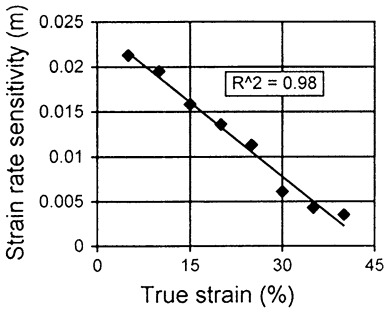

Fig. 7 Variation of strain rate sensitivity (m) with true strain

0.98). The exponents of these power relationships correspond to the SRS (m) of the investigated steel for different constant true strains. Here, it should be importantly noted that consideration of the gradual increase of yield strength and simultaneous lowering of transition strains with increase in strain rate resolves the apparent contradiction of obtaining higher flow stress even with reduced work hardening as the strain rate is increased. On plotting the m values as function of true strain (Fig. 7), it is found that m of the present steel is a linearly decreasing function of true strain (ε) as: $m = -0.0006\varepsilon + 0.0244$.

Now, considering the relationships between dislocation velocity (v) with stress (σ): $v = A\ \sigma^{m'}$, where m' is constant, and, strain rate ($\dot{\varepsilon}$) with mobile dislocation density (ρ) and dislocation velocity (v) together: $\dot{\varepsilon} = b\rho v$, the following equation can be written [31]:

$$1/m = m' + (\delta \ln \rho / \delta \ln \sigma), \quad (1)$$

where m = strain rate sensitivity = $\delta \ln\sigma / \delta \ln\dot{\varepsilon}$

In case there is no change in dislocation density with increasing stress then according to Eq. 1, m' becomes equal to $1/m$. Although it is extremely hard to believe that there is no change in dislocation structure and the associated dislocation density with change in flow stress, this assumption is made in finding SRS from strain rate jump test at fixed temperature and strain. In the present study, it is observed that $1/m$ varies with true strain (ε) as an exponentially increasing function as shown in Fig. 8a. Extrapolation of these data trend ($1/m$, ε) at $\varepsilon = 0.0$ gives an estimation

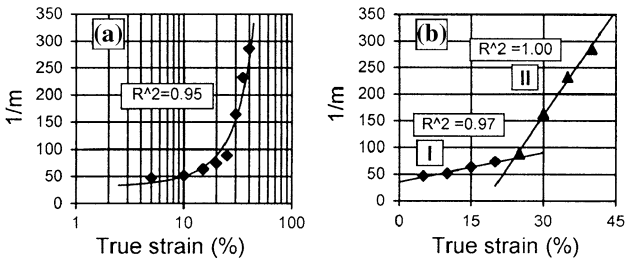

Fig. 8 Variation of the reciprocal of strain rate sensitivity ($1/m$) with true strain: **a** semi-logarithmic plot and **b** linear plot

for m' as 29.44 relating dislocation velocity with stress ($v = A{\cdot}\sigma^{m''}$). However, two perfectly linear segments are obtained when the same data set is plotted on linear scale (Fig. 8b). Extrapolation of the first segment at $\varepsilon = 0.0$ gives the value of m' as 36; while in literature [31] m' value for iron is reported as 38. The m' value (29 or 36) so obtained in the present study seems to be a reasonably good estimation for the present steel.

The appearance of the second linear segment commencing at $\sim$25% strain with much higher slope (Fig. 7b) is attributed to the additional generation of dislocations associated with the formation of DIM. Quite interestingly this transition occurs at a strain ($\sim$25%) above which Stage-III deformation controlled by DIM occurs for all strain rates. Talonen et al. [4] observed that flow stress in 301LN steel obeyed a linear relationship with square root of martensite volume fraction and the slope of this linear relationship abruptly changed (increased) at about 30% martensite. As it is well known that flow stress in any material linearly depends on the square root of dislocation density and also the relationship holds good in presence of DIM [32], it is suggested that the linear variation of flow stress with square root of martensite content is an indirect effect of martensite formation on flow stress through increased density of geometrically necessary dislocations in austenite. The change in slope (increase) as observed by Talonen et al. at $\sim$30% martensite bears similarity with the present result shown in Fig. 7b, but in a different way. Considering the observations of Talonen et al. [3] and present results it is proposed that the increased dislocation density in austenite associated with the formation of some critical amount of martensite plays greater role as compared to dislocation velocity in carrying out the imposed strain rate and the amount of deformation necessary for formation of this critical amount of martensite depends upon the imposed strain rate.

Conclusions

The effect of strain rate on quasi-static tensile flow behaviour of solution annealed 304 stainless steels has been studied at room temperature. From "Results and discussion" section presented above, the following conclusions have been drawn.

1. With increase in strain rate yield strength increases, but tensile strength and ductility are decreased. The lowering of tensile strength and ductility with increase in strain rate results from the dominant effect of thermal softening arising out of adiabatic heating over work hardening and for lesser amount of martensite formation.
2. Tensile deformation of solution annealed 304 stainless steel occurs in three stages. The deformation transition strains depend on strain rate in such a manner that planar slip activity (Stage-I) is favoured at lower strain rate.
3. Strain rate sensitivity (m) of the steel is found to decrease linearly with true strain as: $m = -0.0006\varepsilon + 0.0244$.
4. Reasonably good estimation for the stress exponent (m') relating dislocation velocity and stress has been made for the solution annealed 304 steel.
5. Distinctly two different stages of variation for $1/m$ against true strain (ε) revealed on the linear plot suggests that after some critical amount of martensite formation the underlying mechanism for the tensile flow behaviour is changed and controlled by the increased dislocation density in austenite arising out of DIM formation.

References

1. Gallee S, Manach PY, Thuillier S (2007) Mater Sci Eng A 466:47
2. Angel T (1954) J Iron Steel Inst 177:65
3. Talonen J, Nenonen P, Pape G, Hänninen H (2005) Metall Trans A 36:421
4. De AK, Speer GJ, Matlock DK, Murdock DC, Mataya MC, Comstock RJ Jr (2006) Metall Trans A 37:1875
5. Spencer K, Embury JD, Conlon KT, Veron M, Bréchet Y (2004) Mater Sci Eng A 387:873
6. Lichtenfeld JA, Mataya MC, Van Tyne CJ (2006) Metall Trans A 37:147
7. Powell GW, Marshall ER, Backofen WA (1958) ASM Trans Q 50:478
8. Okutani T, Yukawa N, Ishikawa K, Jinma T (1995) Proc Japanese Soc Tech Plast 1995 Spring, May 18–20, Tokyo, p 331
9. Hecker SS, Stout MG, Staudhammer KP, Smith JL (1982) Metall Trans A 13:619
10. Iwamoto T, Tsuta T, Tomita Y (1998) Int J Mech Sci 40:173
11. Bressanelli JP, Moskowitz A (1966) Trans Am Soc Met 59:223
12. Murr LE, Staudhammer KP, Hecker SS (1982) Metall Trans A 13:627
13. Lee WS, Lin CF (2001) Mater Sci Eng A 308:124
14. Milititsky M, Wispelaere ND, Petrov R, Ramos JE, Reguly A, Hänninen H (2008) Mater Sci Eng A 498:289

15. Picu RC, Vincze G, Ozturk F, Gracio JJ, Barlat F, Maniatty AM (2005) Mater Sci Eng A 390:334
16. Stuwe HP, Les P (1998) Acta Mater 46:6375
17. Chiou ST, Cheng WC, Lee WS (2005) Mater Sci Eng A 392:156
18. Wang Y, Zhou Y, Xia Y (2004) Mater Sci Eng A 372:186
19. Uenishi A, Teodosiu C (2003) Acta Mater 51:4437
20. Ganesh Sundar Raman S, Padmanabhan KA (1994) Mater Sci Technol 10:610
21. Das A, Sivaprasad S, Ghosh M, Chakraborti PC, Tarafder S (2008) Mater Sci Eng A 486:283
22. Das A, Sivaprasad S, Chakraborti PC, Tarafder S (2008) Mater Sci Eng A 496:98
23. Feaugas X (1999) Acta Mater 47:3617
24. Feaugas X, Haddou H (2003) Metall Trans A 34:2329
25. Flinn JE, Field DP, Korth GE, Lillo TM, Macheret J (2001) Acta Mater 49:2065
26. Narutani T, Takamura J (1991) Acta Metall Mater 39:2037
27. Byun TS, Hashimoto N, Farrell K (2004) Acta Mater 52:3889
28. Fang XF, Dahl W (1991) Mater Sci Eng A 141:189
29. Lee TH, Oh CS, Kim SJ (2008) Scr Mater 58:110–113
30. Bracke L, Kestens L, Penning J (2007) Scr Mater 57:385
31. Dieter GE (1988) Mechanical metallurgy, SI metric edn. McGraw-Hill, London
32. Narutani T (1989) Mater Trans JIM 30:33